Modeling Selenite Adsorption Envelopes on Oxides, Clay Minerals, and Soils using the Triple Layer Model

Sabine Goldberg*
USDA-ARS
U.S. Salinity Lab.
450 W. Big Springs Rd.
Riverside, CA 92507

Selenite adsorption behavior was investigated on amorphous Al and Fe oxides, clay minerals: kaolinite, montmorillonite, and illite, and 45 surface and subsurface soil samples from the southwestern and midwestern regions of the United States as a function of solution pH. Selenite adsorption decreased with increasing solution pH. The triple layer model, a chemical surface complexation model, was able to describe selenite adsorption as a function of solution pH by simultaneously optimizing both inner-sphere and outer-sphere selenite surface complexation constants. The fit of the triple layer model to selenite adsorption by soils was much improved over that obtained previously by optimizing solely an inner-sphere selenite surface complexation constant and the protonation constant in the constant capacitance model. In this previous application, the deprotonation constant had been neglected; thereby, preventing the reactive surface hydroxyl group from deprotonating; a chemically unrealistic situation. The selenite surface speciation predicted using the triple layer model was in agreement with that obtained for other strongly adsorbing anions such as molybdate. Direct spectroscopic investigations of selenite surface configuration are needed to corroborate the species predicted by the modeling approach.

Selenium is an essential micronutrient element for animals. The concentration range between deficiency and toxicity is very narrow. Elevated concentrations of Se in soils and waters can occur as a result of discharge from petroleum refineries and mining operations, disposal of fly ash and coal ash, and mineral oxidation and dissolution (Girling, 1984). Vegetation grown on seleniferous soils can become toxic to grazing animals (Lakin, 1961). Deaths and deformities of migratory waterfowl have been attributed to elevated concentrations of Se in agricultural drainage waters (Ohlendorf et al., 1986). In soil solution, the dominant inorganic Se species are: selenate, Se(VI), under oxidizing conditions and selenite, Se(IV), under more reducing conditions (Adriano, 1986). Selenate is considered to be the less toxic oxidation state (Fernandez et al., 1993). Redox transformation rates for inorganic Se species are slow so that both selenate and selenite often coexist in soil solution (Masscheleyn et al., 1990).

Selenium adsorption has been investigated on a wide range of surfaces including: aluminum and iron oxides, clay minerals, and whole soils. Soil constituents that are significantly positively correlated with soil Se content include: extractable Al and Fe oxides and clay minerals (Lévesque, 1974). Selenate has been observed to adsorb to a much lesser extent than selenite on goethite (Balistrieri and Chao, 1987), hematite (Duc et al., 2003), and soils (Neal and Sposito, 1989). Sorption of both Se redox states on Fe oxides was greatest at pH 3 and decreased with increasing solution pH (Balistrieri and Chao, 1987; Parida et al., 1997; Duc et al., 2003). Selenite adsorption on a disordered Al hydroxide decreased as pH was

Soil Sci. Soc. Am. J. 77:64–71
doi:10.2136/sssaj2012.0205
Contribution from the U.S. Salinity Laboratory.
Received 28 June 2012.
*Corresponding author (Sabine.Goldberg@ars.usda.gov).

increased from 5 to 10 (Papelis et al., 1995). Selenite adsorption on kaolinite, smectite, and illite exhibited adsorption maxima in the pH range 3 to 5 and decreased with increasing solution pH (Goldberg and Glaubig, 1988; Missana et al., 2009). Similar to the behavior on Fe and Al oxides and clay minerals, selenite adsorption on soils from California, Iowa, Oklahoma, and South Dakota decreased with increasing soil solution pH (Neal et al., 1987; Goldberg and Glaubig, 1988; Goldberg et al., 2007; Lee et al., 2011).

Evidence for strong specific adsorption of selenite as an inner-sphere surface complex containing no water between the adsorbing ion and the surface functional group has been provided by point of zero charge shifts observed using electrophoretic mobility measurements for alumina (Rajan, 1979), goethite, and amorphous Fe oxide (Su and Suarez, 2000). Additional macroscopic evidence for inner-sphere surface complex formation of selenite was found by its lack of ionic strength dependence in adsorption behavior as seen for amorphous Fe oxide, goethite, hematite (Su and Suarez, 2000; Duc et al., 2003), and for the clay minerals, illite and smectite (Missana et al., 2009).

Direct spectroscopic evidence for specific inner-sphere surface complexation of selenite has been observed on goethite, hematite, amorphous Fe oxide (Hayes et al., 1987; Manceau and Charlet, 1994; Catalano et al., 2006), and on the clay mineral, montmorillonite (Peak et al., 2006). Selenate, which is generally considered to be the more weakly held inorganic Se species, was observed to form both inner- and outer-sphere surface complexes on goethite and Al oxide using vibrational spectroscopies (Wijnja and Schulthess, 2000). Simultaneous formation of both inner- and outer-sphere surface complexes was also observed spectroscopically for arsenite adsorption (Arai et al., 2001) and molybdate adsorption (Goldberg et al., 2008a) on Al oxide. Somewhat surprisingly, even strongly adsorbing anions have been observed to form mixtures of inner-sphere and outer-sphere surface complexes. On amorphous Al oxide, selenite was observed to form primarily inner-sphere but also some outer-sphere surface complexes (Peak, 2006). Arsenate, a very strongly adsorbing anion, was found to adsorb simultaneously as inner- and outer-sphere surface species on hematite and Al oxide using X-ray scattering measurements (Catalano et al., 2008).

Selenite adsorption on soils and soil minerals has been described using various chemical surface complexation modeling approaches. Such models include the constant capacitance model (Goldberg, 1985; Sposito et al., 1988; Goldberg and Glaubig, 1988; Anderson and Benjamin, 1990a, 1990b; Duc et al., 2003, 2006; Goldberg et al., 2007, 2008b), the diffuse layer model (Dzombak and Morel, 1990; Balistrieri et al., 2003; Jordan et al. (2009a, 2009b); Kim et al., 2012), the triple layer model (Hayes et al., 1988; Balistrieri and Chao, 1990; Zhang and Sparks, 1990; Ghosh et al., 1994; Martinez et al., 2006; Rovira et al., 2008), and the CD-MUSIC model (Hiemstra and van Riemsdijk, 1999; Hiemstra et al., 2007). All of the surface complexation modeling studies postulated inner-sphere surface complexes for selenite absorption. Unlike adsorption isotherm equations, whose parameters are usually empirical and valid only for the conditions under which the experiment was conducted, surface complexation models define specific surface species, chemical reactions, mass balances, and charge balances. They contain molecular features such as, surface activity coefficients and surface complexation equilibrium constants, that can be given thermodynamic significance (Sposito, 1983).

The constant capacitance model was applied to describe selenite adsorption by the clay minerals: kaolinite and montmorillonite (Goldberg and Glaubig, 1988) and soils (Sposito et al., 1988; Goldberg and Glaubig, 1988). The predictive ability of the constant capacitance model to describe selenite adsorption by soils has been evaluated previously (Goldberg et al., 2007). General regression equations were developed to predict model selenite surface complexation constants from easily measured soil physical properties: surface area, organic C content, inorganic C content, Al oxide content, and Fe oxide content. These predicted constants were then used in the constant capacitance model to successfully predict selenite adsorption on additional soils. Therefore, this study provided a completely independent evaluation of the predictive capability of the constant capacitance model to describe selenite adsorption by soils. The surface complexation constants used in the predictive study were the protonation constant for the reactive surface hydroxyl group and a formation constant for a monodentate negatively charged selenite surface species. The deprotonation constant was neglected after preliminary model results indicated that it was required only in trace amounts (Goldberg et al., 2007). However, not allowing deprotonation of the reactive surface functional group is not very realistic. Surface complexation modeling of Mo adsorption by amorphous Al and Fe oxide and by a diverse set of soils was successful using both an inner-sphere and an outer-sphere surface complex in the triple layer model (Goldberg et al., 2008a). This surface speciation was in agreement with that observed by the same authors on amorphous Al oxide using vibrational spectroscopy.

The objectives of the present study were: (i) to determine selenite adsorption on amorphous Al and Fe oxide and the clay minerals: kaolinite, montmorillonite, and illite as a function of solution pH; and (ii) to test the ability of the triple layer model to describe selenite adsorption on these oxides and clay minerals, as well as on the 45 soil samples previously used in the predictive study of Goldberg et al. (2007), using both inner-sphere and outer-sphere surface configurations.

MATERIALS AND METHODS

Selenite adsorption behavior was studied on various adsorbents. Amorphous Al and Fe oxide were synthesized according to the procedure of Sims and Bingham (1968). X-ray diffraction analyses using powder mounts verified that the oxides were amorphous and contained no detectable crystalline impurities. Samples of kaolinite (KGa-2, poorly crystallized Georgia kaolinite), Na-montmorillonite (SWy-1, Wyoming bentonite), and IMt-2 illite (Silver Hill illite) were obtained

from the Clay Minerals Society's Source Clay Repository (Purdue University, West Lafayette, IN). The kaolinite and montmorillonite were used without any pretreatment. The illite was ground using a mortar and pestle to pass a 0.05-mm sieve. X-ray diffraction analyses using powder mounts found traces of chlorite in the kaolinite, traces of mica in the montmorillonite, and traces of kaolinite and vermiculite in the illite. Surface areas of the oxides and clays, determined using a single-point BET N_2 adsorption isotherm, were: 25.6 $m^2\ g^{-1}$ for Al oxide, 158 $m^2\ g^{-1}$ for Fe oxide, 20.8 $m^2\ g^{-1}$ for kaolinite, 24.8 $m^2\ g^{-1}$ for montmorillonite, and 23.1 $m^2\ g^{-1}$ for illite.

Selenite adsorption envelopes [amount of Se(IV) adsorbed as a function of solution pH per fixed total Se(IV) concentration] were determined in batch systems. Samples of adsorbent (0.25 g for Fe oxide, 0.5 g for Al oxide, and 1.2 g for clays) were equilibrated with aliquots (200 mL for Fe oxide, 100 mL for Al oxide, and 30 mL for clays) of 0.1 M NaCl background electrolyte solution for 2 h on a reciprocating shaker. The equilibrating solution also contained 20 μmol Se(IV) L^{-1} and had been adjusted to the desired pH range with 1 M HCl or 1 M NaOH additions that changed the total volume by < 2%. After reaction, the samples were centrifuged, decanted, analyzed for pH, filtered through 0.45-μm membrane filters, and analyzed for Se concentration using inductively coupled plasma optical emission spectrometry. Selenite adsorption envelopes on the <2-mm fraction of 45 soil samples from 36 soil series belonging to six different soil orders had been determined previously as described by Goldberg et al. (2007). The soils represented a wide range of chemical characteristics and soil classifications as shown in Table 1 of Goldberg et al. (2007). The analytical methods used to characterize the soil samples are described and referenced in this publication. The average values of various soil chemical properties: cation exchange capacity, inorganic C content, organic C content, Fe oxide content, Al oxide content, and surface area were not statistically significantly different at the 95% level of confidence for the 23 southwestern soils vs. the 22 midwestern soils.

The ability of the constant capacitance model to describe and predict selenite adsorption on 45 soil samples was evaluated previously using an inner-sphere adsorption mechanism. Surface complexation reactions, surface complexation constants, mass balance, and charge balance expressions are provided in Goldberg et al. (2007). The present study investigates the use of a combination of inner-sphere and outer-sphere surface complexes in the triple layer model to describe selenite adsorption by oxides and clay minerals and tests whether this approach provides a superior fit to selenite adsorption by the soil samples. Despite the fact that both monodentate and bidentate selenite surface complexes have been observed on metal oxide surfaces (Peak, 2006; Foster et al., 2003), the vast majority of surface complexation modeling approaches have used monodentate complexes. Therefore, for the sake of consistency with the previous investigation of Goldberg et al. (2007), and to minimize the number of adjustable parameters, the current application was restricted to monodentate surface complexes. A detailed discussion of the theory and assumptions of the triple layer model are provided in Goldberg (1992). In the present application of the triple layer model, the following surface complexation reactions for adsorbed Se(IV) are considered:

$$SOH_{(s)} + H_2SeO_{3(aq)} \leftrightarrow SHSeO_{3(s)} + H_2O \quad [1]$$

$$SOH_{(s)} + H_2SeO_{3(aq)} \leftrightarrow SOH_2^+ - HSeO_{3(s)}^- \quad [2]$$

$$SOH_{(s)} + H_2SeO_{3(aq)} \leftrightarrow SOH_2^+ - SeO_{3(s)}^{2-} + H_{(aq)}^+ \quad [3]$$

where $SOH_{(s)}$ represents reactive surface hydroxyl groups on oxide minerals, FeOH or AlOH, and aluminol groups, AlOH, on the edges of clay minerals. Equilibrium constant expressions for the above Se(IV) surface complexation reactions are:

$$K_{Se}^{1is}(\text{int}) = \frac{[SHSeO_3]}{[SOH][H_2SeO_3]} \quad [4]$$

$$K_{Se}^{1os}(\text{int}) = \frac{[SOH_2^+ - HSeO_3^-]}{[SOH][H_2SeO_3]} \exp\left[F(\psi_o - \psi_\beta)/RT\right] \quad [5]$$

$$K_{Se}^{2os}(\text{int}) = \frac{[SOH_2^+ - SeO_3^{2-}][H^+]}{[SOH][H_2SeO_3]} \exp\left[F(\psi_o - 2\psi_\beta)/RT\right] \quad [6]$$

where square brackets indicate concentrations (mol L^{-1}), F is the Faraday constant (C mol_c^{-1}), ψ_o is the surface potential (V) in the o-plane of inner-sphere (*is*) adsorption, ψ_β is the surface potential (V) in the β-plane of outer-sphere (*os*) adsorption, R is the molar gas constant (J $mol^{-1}\ K^{-1}$), and T is the absolute temperature (K). The exponential terms can be considered as solid-phase activity coefficients that correct for the charges on the surface complexes located in each surface plane of adsorption.

The mass balance equation for the surface functional group is:

$$[SOH]_T = [SOH] + [SOH_2^+] + [SO^-] + [SO^- - Na^+] + [SOH_2^+ - Cl^-] + [SHSeO_3] + [SOH_2^+ - HSeO_3^-] + [SOH_2^+ - SeO_3^{2-}] \quad [7]$$

and the charge balance equations are:

$$\sigma_o + \sigma_\beta + \sigma_d = 0 \quad [8]$$

$$\sigma_o = [SOH_2^+] + [SOH_2^+ - Cl^-] - [SO^-] - [SO^- - Na^+] + [SOH_2^+ - HSeO_3^-] + [SOH_2^+ - SeO_3^{2-}] \quad [9]$$

$$\sigma_\beta = [SO^- - Na^+] - [SOH_2^+ - Cl^-] - [SOH_2^+ - HSeO_3^-] - 2[SOH_2^+ - SeO_3^{2-}] \quad [10]$$

where the σ_i have units of ($mol_c\ L^{-1}$).

The computer program FITEQL 4.0 (Herbelin and Westall, 1999) was used to fit selenite surface complexation constants to the experimental adsorption data of Goldberg et al. (2007). The program uses a nonlinear least squares optimization routine to fit equilibrium constants to experimental data and contains the triple layer model for surface complexation. Soils are complex multi-site mixtures containing many diverse surface sites. Therefore, the assumption that selenite adsorption takes place on only one set of reactive surface functional groups is a gross

simplification and the selenite surface complexation constants obtained for soils are average composite values that include soil mineralogical characteristics and competing ion effects.

Initial input parameter values for the triple layer model were: surface area, total number of reactive surface hydroxyl groups: N_S = 2.31 sites nm^{-2} (recommended for natural materials by Davis and Kent, 1990), capacitances: C_1 = 1.2 F m^{-2}, C_2 = 0.2 F m^{-2} (considered optimum for goethite by Zhang and Sparks, 1990), protonation constant: $\log K_+(int)$ = 5.0, dissociation constant: $\log K_-(int)$ = −11.2, background electrolyte constants: $\log K_{Na}^{+}(int)$ = −8.6, $\log K_{Cl}^{-}(int)$ = 7.5 (from Sprycha, 1989a, 1989b) for amorphous Al oxide, clay minerals, and soils and protonation constant: $\log K_+(int)$ = 4.3, dissociation constant: $\log K_-(int)$ = −9.8, background electrolyte constants: $\log K_{Na}^{+}(int)$ = −9.3, $\log K_{Cl}^{-}(int)$ = 5.4 (from Zhang and Sparks, 1990) for amorphous Fe oxide. This set of parameter values has been used in previous applications of the triple layer model to anion adsorption by soils (Goldberg et al., 2008a; Goldberg and Kabengi, 2010). Goodness-of-fit was evaluated using the overall variance parameter, V, in the dependent variable, Y:

$$V_Y = \frac{SOS}{DF} \qquad [11]$$

where SOS is the weighted sum of squares of the residuals and DF is the degrees of freedom.

RESULTS AND DISCUSSION

Selenite adsorption as a function of solution pH is indicated in Fig. 1 for amorphous Al and Fe oxide and the clay minerals, kaolinite and illite. On the oxide minerals (Fig. 1a and 1b), selenite adsorption exhibited a broad maximum up to pH 8 and then decreased rapidly with increasing solution pH. Similar pH-dependent adsorption behavior had been observed previously for selenite on amorphous Fe oxide by Balistrieri and Chao (1987). Selenite adsorption on the clay minerals increased at low solution pH, exhibited adsorption maxima near pH 5 for kaolinite and pH 4 for illite, and decreased at higher solution pH value (Fig. 1c and 1d). Similar parabolic adsorption behavior had been observed previously for selenite adsorption on the clay minerals, kaolinite and montmorillonite (Goldberg and Glaubig, 1988). The decrease in selenite adsorption observed below pH 3 for kaolinite and illite may be due to clay mineral dissolution.

The ability of the triple layer model to describe selenite adsorption on amorphous Al and Fe oxide is depicted in Fig. 1a and 1b. For amorphous Al oxide, the model described the data quantitatively over the entire pH range (3.5–9.5) investigated; while for amorphous Fe oxide, the model description was quantitative at values ≤pH 7 and ≥pH 10. In the intermediate range, 8 ≤ pH ≤ 9.5, the model description deviated from the experimental data by at most 10%. With the exception of a <5% deviation at the point of the adsorption maximum, the model was able to describe selenite adsorption on illite over the entire solution pH range investigated (Fig. 1d). For selenite adsorption on kaolinite, the magnitude of the adsorption maximum was well described but deviations in model fit were observed in the range 3 ≤ pH ≤ 8 (Fig. 1c). Table 1 provides values for the optimized selenite surface complexation constants.

The selenite surface speciations obtained from the triple layer model are presented in Fig. 2 and Fig. 3. For the oxide minerals (Fig. 2), the inner-sphere surface complex predominates at low and intermediate solution pH and the outer-sphere surface complex dominates only at high pH. This is in agreement with the spectroscopic results of Wijnja and Schulthess (2000) for selenate adsorption on goethite. Additionally, the modeled pH-dependent distribution of inner-sphere vs. outer-sphere surface selenite complexes is in excellent agreement with the one obtained by the triple layer model for molybdate adsorption on these same amorphous oxide minerals (Goldberg et al., 2008a). As had been the case for molybdate adsorption, the triple layer model predicted a larger proportion of outer-sphere surface selenite complexes over a larger solution pH range for amorphous Al oxide (Fig. 2a) than for amorphous Fe oxide (Fig. 2b). An increased propensity for anions to form outer-sphere surface complexes on Al oxide as compared to Fe oxide has been observed previously, suggesting stronger anion adsorption on Fe oxide (Goldberg and Johnston, 2001; Peak, 2006).

For the clay minerals, the triple layer model described selenite adsorption using predominately outer-sphere surface complexes such that the inner-sphere complex was present in trace amounts for illite (Fig. 3b) and not even necessary to produce model convergence for kaolinite (Fig. 3a). These results would suggest that selenite is adsorbed less strongly on clay minerals than on oxides, in agreement with their much lower total amount of adsorption observed on a per gram, as well as on a per meter squared basis. The optimized values for the selenite surface complexation constants are provided in Table 1.

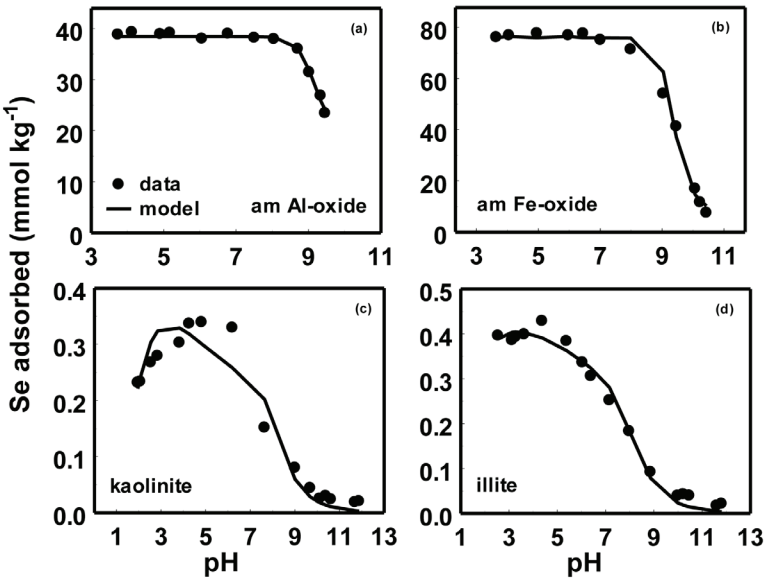

Fig. 1. Fit of the triple layer model to Se(IV) adsorption on oxides and clay minerals: (a) amorphous Al oxide, (b) amorphous Fe oxide, (c) kaolinite, (d) illite. Experimental data are represented by circles. Model fits are represented by lines.

Table 1. Triple layer model Se(IV) surface complexation constants.

Solid	Soil description	LogK^{1is}_{Se}	LogK^{1os}_{Se}	LogK^{2os}_{Se}	SOS/DF†
Oxides					
Amorphous Al oxide		13.31		8.73	0.04
Amorphous Fe oxide		12.76		4.32	0.4
Clay minerals					
KGa-2 kaolinite			7.21	0.616	1.4
SWy-1 montmorillonite			6.53	0.369	0.4
IMt-2 illite		2.76	7.53	0.629	0.6
Soils					
Altamont clay loam	fine, smectitic, thermic Aridic Haploxerert	2.72	5.29	–0.727	0.8
Arlington loam	coarse-loamy, mixed active, thermic Haplic Durixeralf	2.99	5.99	–0.605	0.3
Avon silt loam	fine, smectitic, mesic calcic Pachic Argixeroll	2.48	5.62	–0.534	0.3
Bonsall clay loam	fine, smectitic, thermic Natric Palexeralf	3.26	6.04	–0.389	0.4
Chino clay loam	fine-loamy, mixed, superactive, thermic Aquic Haploxeroll	2.10	5.09	–1.47	0.6
Diablo clay	fine, smectitic, thermic Aridic Haploxerert	2.04	5.10	–0.826	0.4
Diablo clay loam		2.08	4.57	–1.24	1.3
Fallbrook loamy sand	fine-loamy, mixed, superactive, thermic Typic Haploxeralf	3.25	6.17	–0.108	0.3
Fiander clay loam	fine-silty, mixed superactive, mesic Typic Natraquoll	2.53	5.59	–1.08	0.7
Hanford loam	coarse-loamy, mixed, superactive, nonacid thermic Typic Xerorthent	3.42	6.36	0.209	2.1
Haines silt loam	coarse-silty, mixed, superactive, calcareous, mesic Typic Endoaquept			–0.642	5.4
Holtville sandy loam	clayey over loamy, smectitic over mixed, superactive, calcareous, hyperthermic Typic Torrifluvent	3.73	5.45	–0.286	2.4
Imperial clay	fine, smectitic, calcareous, hyperthermic Vertic Torrifluvent	3.92		–0.626	3.0
Nohili silt loam	very-fine, smectitic, calcareous, isohyperthermic Cumulic Endoaquoll	1.17	5.52	–0.489	4.9
Pachappa loam	coarse-loamy, mixed, active, thermic Mollic Haploxeralf	2.57	5.32	–1.06	2.2
Pachappa sandy loam 0–25 cm		3.36	6.17	0.0226	0.4
Pachappa sandy loam 25–51 cm		3.35	6.47	–0.0591	1.8
Porterville silty clay loam	fine, smectitic, thermic Aridic Haploxerert	3.13	5.82	–0.486	0.3
Reagan clay loam	fine-silty, mixed superactive, thermic Ustic Haplocalcid	3.38		–0.589	7.9
Sebree silt loam	fine-silty, mixed, superactive, mesic Xeric Natridurid	3.20	6.39	0.105	0.7
Wasco sandy loam	coarse-loamy, mixed, superactive, nonacid, thermic Typic Torriorthent	1.99	5.80	–0.329	1.3
Wyo silt loam	fine-loamy, mixed, thermic Mollic Haploxeralf	3.53	6.36	–0.0753	0.6
Yolo loam	fine-silty, mixed, superactive, nonacid, thermic Mollic Xerofluvent	3.65	6.29	–0.386	0.3
Bernow	fine-loamy, siliceous, active, thermic Glossic Paleudalf	7.07		1.02	0.2
Canisteo	fine-loamy, mixed, superactive, calcareous, mesic Typic Endoaquoll	3.36	4.92	–0.815	3.9
Dennis A	fine, mixed, active, thermic Aquic Argiudoll	4.71	7.01	0.979	0.3
Dennis B		10.59		1.14	0.3
Dougherty	loamy, mixed, active, thermic Arenic Haplustalf	1.88	4.88	–1.10	0.2
Hanlon	coarse-loamy, mixed, superactive, mesic Cumulic Hapludoll	2.86	6.09	–0.446	0.3
Kirkland	fine, mixed, superactive, thermic Udertic Paleustoll	2.77	6.07	0.0192	1.9
Luton	fine, smectitic, mesic Typic Endoaquert	3.09	5.99	–0.111	1.7
Mansic A	fine-loamy, mixed, superactive, thermic Aridic Calciustoll	4.36		–0.473	3.5
Mansic B		4.47		–0.0375	10.7
Norge	fine-silty, mixed, active, thermic Udic Paleustoll	2.88	6.18	–0.0176	1.1
Osage A	fine, smectitic, thermic Typic Epiaquert	4.64	6.96	0.428	0.2
Osage B		2.32	5.91	–0.304	4.9
Pond Creek A	fine-silty, mixed, superactive, thermic Pachic Argiustoll	2.74	5.88	–0.253	0.8
Pond Creek B		2.54	6.17	–0.138	1.4
Pratt A	sandy, mixed, mesic Lamellic Haplustalf	2.66	5.51	–0.603	0.1
Pratt B		1.62	4.81	–1.22	0.1
Richfield	fine, smectitic, mesic Aridic Argiustoll	2.97	6.09	–0.190	0.8
Summit A	fine, smectitic, thermic oxyaquic Vertic Argiudoll	3.69	6.80	0.131	0.4
Summit B		7.11		0.621	0.2
Taloka	fine, mixed, active, thermic Mollic Albaqualf	3.03	5.99	–0.296	0.5
Teller	fine-loamy, mixed, active, thermic Udic Argiustoll	2.21	5.37	–0.928	0.7
Soil average log*K*(int)		3.35	5.84	–0.317	
Standard deviation		1.61	0.59	0.579	

† SOS, sum of squares; DF, degrees of freedom.

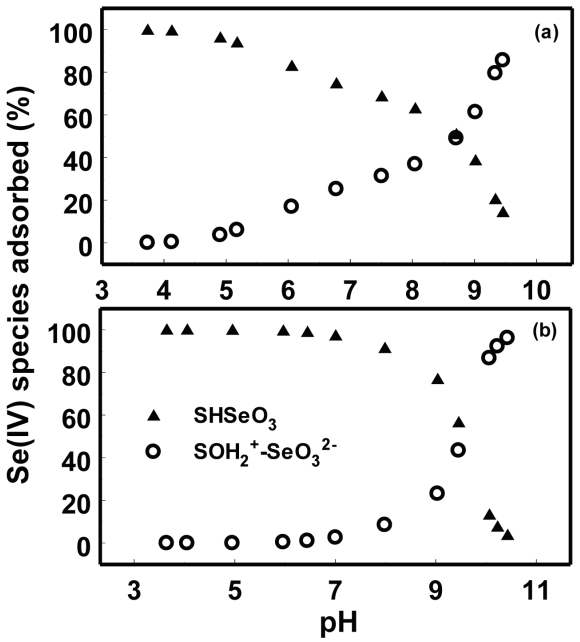

Fig. 2. Surface speciation predicted by the triple layer model for Se(IV) adsorption on oxides: (a) amorphous Al oxide, (b) amorphous Fe oxide.

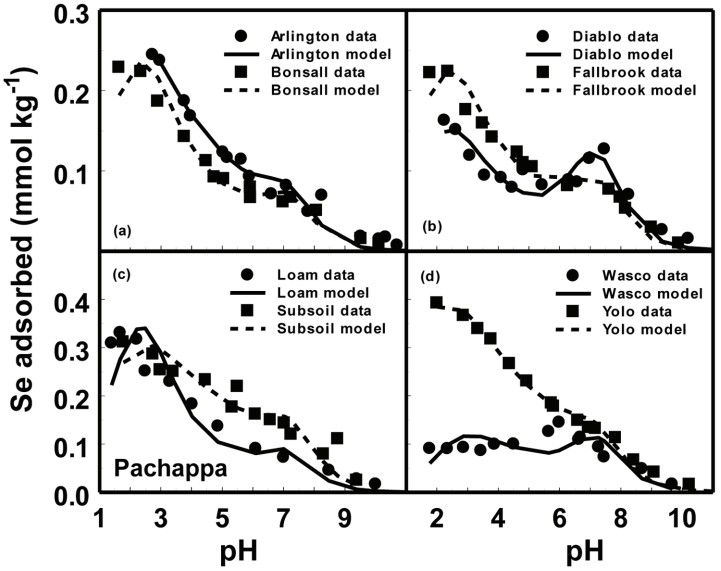

Fig. 4. Fit of the triple layer model to Se(IV) adsorption on southwestern soils. Experimental data are represented by solid symbols. Model fits are represented by lines.

Selenite adsorption as a function of solution pH had been determined previously for 45 different soil samples including a subgroup of 23 soils primarily from the southwestern United States and a subgroup of 22 soils from the Midwest, specifically Iowa and Oklahoma (Goldberg et al., 2007). Figures 4 and 5 depict the selenite adsorption data previously presented in Fig. 1 and 2 of Goldberg et al. (2007) for southwestern and midwestern soils, respectively. Selenite adsorption was found to be maximal at acid pH and to decrease rapidly with increasing solution pH. The decrease in selenite adsorption commenced at a much lower solution pH value for the southwestern soils (Fig. 4) than for the midwestern soils (Fig. 5). The constant capacitance model was well able to fit the selenite adsorption envelopes on all of the soil samples, but increasing underprediction was observed above pH 8 (see Fig. 1 and 2 of Goldberg et al., 2007). Similar underprediction at high solution pH had been encountered by Goldberg et al. (2002) in describing molybdate adsorption on 36 similar soil samples using the constant capacitance model. Reanalysis of the data of Goldberg et al. (2002) with the triple layer model and including both an inner-sphere and an outer-sphere molybdate surface complexation constant provided a much improved fit, especially at high solution pH (Goldberg et al., 2008a).

The present application of the triple layer model to describe selenite adsorption using both inner-sphere and outer-sphere surface configurations led to similar improvement at high pH over the

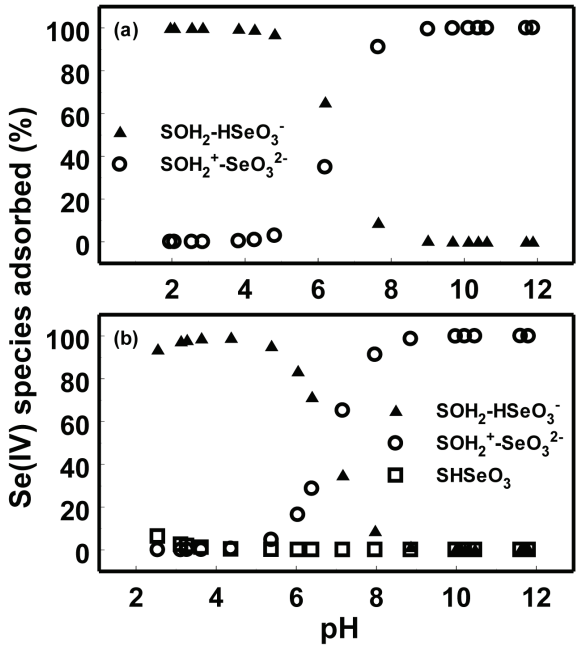

Fig. 3. Surface speciation predicted by the triple layer model for Se(IV) adsorption on clay minerals: (a) kaolinite, (b) illite.

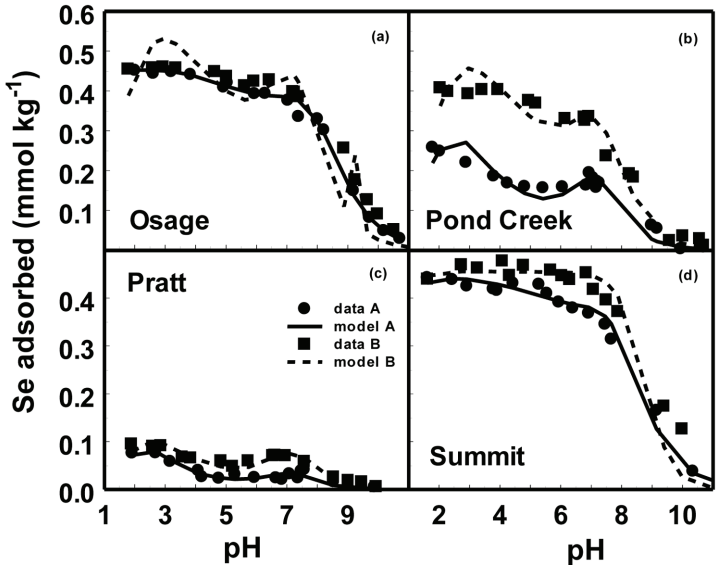

Fig. 5. Fit of the triple layer model to Se(IV) adsorption on midwestern soils: (a) Osage soil, (b) Pond Creek soil, (c) Pratt soil, and (d) Summit soil. Experimental data are represented by circles for the A horizons and by squares for the B horizons. Model fits are represented by solid lines for the A horizons and dashed lines for the B horizons.

previous constant capacitance model application. The triple layer model was optimized using a monodentate inner-sphere surface species, Eq. [1], as previously included in the constant capacitance model (Goldberg et al., 2007). However, two monodentate outer-sphere surface complexes, Eq. [2] and [3], were optimized rather than the protonation constant. As can be seen from Fig. 4 and 5, the triple layer model fit at high solution pH is much improved over the constant capacitance model (Fig. 1 and 2 of Goldberg et al., 2007), especially for the southwestern soils. Some of the improvement in fit must be attributed to the fact that three surface complexation constants rather than two were optimized. However, retaining the deprotonation constant in the triple layer model representation, thereby allowing deprotonation of the surface functional group, rather than removing this constant and preventing deprotonation, as in the previous constant capacitance model application (Goldberg et al., 2007), results in a much more chemically realistic depiction of the soil-solution interface. The reduction in quality of model fit at values below pH 2 is likely due to mineral dissolution.

Optimized selenite surface complexation constants for all soils are provided in Table 1. Average values of the selenite surface complexation constants for the southwestern soils are not statistically significantly different from those for the midwestern soils at the 95% level of confidence. For this reason, general soil average logK(int) values along with their standard deviations are presented in Table 1.

Selenite surface speciations obtained with the triple layer model for one representative southwestern soil, Arlington (Fig. 6a), and one representative midwestern soil, Osage A (Fig. 6b), indicate that the two outer-sphere surface complexes predominate over most of the solution pH range. The inner-sphere surface complex predominates only at solution pH $\leq$ 3 for the Arlington soil and pH $\leq$ 4 for the Osage A soil. Since the selenite adsorbing sites of soils are expected to be a mixture of oxides and clay minerals, it is not surprising that the proportion of inner-sphere and outer-sphere surface complexes is intermediate between these two types of reference minerals. According to the model speciation, selenite adsorption occurs predominantly as an inner-sphere surface complex at low solution pH; while at intermediate and high pH, where the absolute amount of adsorption becomes much reduced, selenite adsorption occurs almost exclusively as outer-sphere surface complexes. The oxide content of the Osage A soil is approximately twice as great as that of the Arlington soil. This is consistent with the greater proportion of the inner-sphere surface complex found on the Osage A soil at low solution pH using the triple layer model.

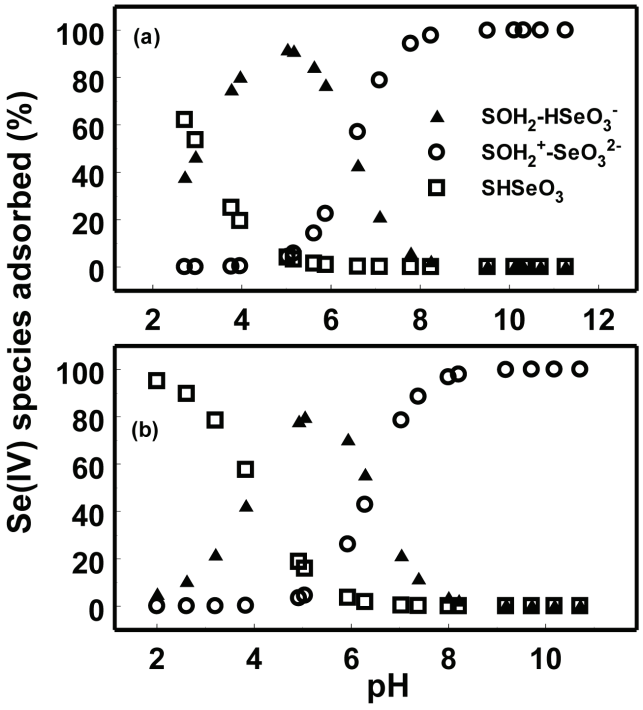

Fig. 6. Surface speciation predicted by the triple layer model for Se(IV) adsorption on soils: (a) Arlington soil, (b) Osage A soil.

Direct spectroscopic experimental evidence is necessary to verify the selenite surface complexes suggested by our indirect modeling results. Incorporation of such molecular-scale experimental information into the macroscopic triple layer model will improve its ability to describe selenite adsorption data on oxides, clay minerals, and soils. The current study was performed at constant selenite concentration and did not evaluate the effect of increasing selenite solution concentration. In the case of B adsorption, surface complexation model parameters developed for B adsorption envelopes on these southwestern soils could be used to describe B adsorption isotherms on these midwestern soils (Goldberg et al., 2004). Therefore, although the effect of selenite loading remains to be investigated, it may be possible to use the triple layer model parameters from the present application to successfully describe selenite adsorption isotherms on soils.

ACKNOWLEDGMENTS

Gratitude is expressed to Ms. P. Xiong for technical assistance.

REFERENCES

Adriano, D.C. 1986. Trace elements in the terrestrial environment. Springer-Verlag, New York.

Anderson, P.R., and M.M. Benjamin. 1990a. Constant capacitance surface complexation model. Adsorption in silica-iron binary oxide suspensions. ACS Symp. Ser. 416:272–281. doi:10.1021/bk-1990-0416.ch021

Anderson, P.R., and M.M. Benjamin. 1990b. Modeling adsorption in aluminum—iron binary oxide suspensions. Environ. Sci. Technol. 24:1586–1592. doi:10.1021/es00080a020

Arai, Y., E.J. Elzinga, and D.L. Sparks. 2001. X-ray absorption spectroscopic investigation of arsenite and arsenate adsorption at the aluminum oxide-water interface. J. Colloid Interface Sci. 235:80–88. doi:10.1006/jcis.2000.7249

Balistrieri, L.S., S.E. Box, and J.W. Tonkin. 2003. Modeling precipitation and sorption of elements during mixing of river water and porewater in the Coeur d'Alene River basin. Environ. Sci. Technol. 37:4694–4701. doi:10.1021/es0303283

Balistrieri, L.S., and T.T. Chao. 1987. Selenium adsorption by goethite. Soil Sci. Soc. Am. J. 51:1145–1151. doi:10.2136/sssaj1987.03615995005100050009x

Balistrieri, L.S., and T.T. Chao. 1990. Adsorption of selenium by amorphous iron oxyhydroxide and manganese dioxide. Geochim. Cosmochim. Acta 54:739–751. doi:10.1016/0016-7037(90)90369-V

Catalano, J.G., C. Park, P. Fenter, and Z. Zhang. 2008. Simultaneous inner-and outer-sphere arsenate adsorption on corundum and hematite. Geochim. Cosmochim. Acta 72:1986–2004. doi:10.1016/j.gca.2008.02.013

Catalano, J.G., Z. Zhang, P. Fenter, and M.J. Bedzyk. 2006. Inner-sphere adsorption geometry of Se(IV) at the hematite (100)-water interface. J. Colloid Interface Sci. 297:665–671. doi:10.1016/j.jcis.2005.11.026

Davis, J.A., and D.B. Kent. 1990. Surface complexation modeling in aqueous geochemistry. Rev. Mineral. 23:117–260.

Duc, M., G. Lefevre, and M. Fedoroff. 2006. Sorption of selenite ions on hematite. J. Colloid Interface Sci. 298:556–563. doi:10.1016/j.jcis.2006.01.029

Duc, M., G. Lefevre, M. Fedoroff, J. Jeanjean, J.C. Ruchard, F. Monteil-Rivera, J. Dumenceau, and S. Milonjic. 2003. Sorption of selenium anionic species

on apatites and iron oxides from aqueous solutions. J. Environ. Radioact. 70:61–72. doi:10.1016/S0265-931X(03)00125-5

Dzombak, D.A., and F.M.M. Morel. 1990. Surface complexation modeling: Hydrous ferric oxide. John Wiley & Sons, New York.

Fernandez, C.M.G., M.A. Palacios, and C. Camara. 1993. Flow-injection and continuous-flow systems for the determination of Se(IV) and Se(VI) by hydride generation atomic absorption spectrometry with on-line prereduction of Se(VI) to Se(IV). Anal. Chim. Acta 283:386–392. doi:10.1016/0003-2670(93)85248-I

Foster, A.L., G.E. Brown, and G.A. Parks. 2003. X-ray absorption fine structure study of As(V) and Se(IV) sorption complexes on hydrous Mn oxides. Geochim. Cosmochim. Acta 67:1937–1953.

Ghosh, M.M., C.D. Cox, and J.R. Yuan-Pan. 1994. Adsorption of selenium on hydrous alumina. Environ. Prog. 13:79–88. doi:10.1002/ep.670130210

Girling, C.A. 1984. Selenium in agriculture and the environment. Agric. Ecosyst. Environ. 11:37–65. doi:10.1016/0167-8809(84)90047-1

Goldberg, S. 1985. Chemical modeling of anion competition on goethite using the constant capacitance model. Soil Sci. Soc. Am. J. 49:851–856. doi:10.2136/sssaj1985.03615995004900040013x

Goldberg, S. 1992. Use of surface complexation models in soil chemical systems. Adv. Agron. 47:233–329. doi:10.1016/S0065-2113(08)60492-7

Goldberg, S., and R.A. Glaubig. 1988. Anion sorption on a calcareous, montmorillonitic soil—selenium. Soil Sci. Soc. Am. J. 52:954–958. doi:10.2136/sssaj1988.03615995005200040010x

Goldberg, S., and C.T. Johnston. 2001. Mechanisms of arsenic adsorption on amorphous oxides evaluated using macroscopic measurements, vibrational spectroscopy, and surface complexation modeling. J. Colloid Interface Sci. 234:204–216. doi:10.1006/jcis.2000.7295

Goldberg, S., S. Hyun, and L.S. Lee. 2008b. Chemical modeling of arsenic (III, V) and selenium (IV, VI) adsorption by soils surrounding ash disposal facilities. Vadose Zone J. 7:1231–1238. doi:10.2136/vzj2008.0013

Goldberg, S., C.T. Johnston, D.L. Suarez, and S.M. Lesch. 2008a. Mechanism of molybdenum adsorption on soils and soil minerals evaluated using vibrational spectroscopy and surface complexation modeling. In: M.O. Barnett and D.B. Kent, editors, Adsorption of metals by geomedia II: Variables, mechanisms, and model applications. Developments in Earth & Environmental Sciences 7. Elsevier, Amsterdam. p. 235–266.

Goldberg, S., and N.J. Kabengi. 2010. Bromide adsorption by reference minerals and soils. Vadose Zone J. 9:780–786. doi:10.2136/vzj2010.0028

Goldberg, S., S.M. Lesch, and D.L. Suarez. 2002. Predicting molybdenum adsorption by soils using soil chemical parameters in the constant capacitance model. Soil Sci. Soc. Am. J. 66:1836–1842. doi:10.2136/sssaj2002.1836

Goldberg, S., S.M. Lesch, and D.L. Suarez. 2007. Predicting selenite adsorption by soils using soil chemical parameters in the constant capacitance model. Geochim. Cosmochim. Acta 71:5750–5762. doi:10.1016/j.gca.2007.04.036

Goldberg, S., D.L. Suarez, N.T. Basta, and S.M. Lesch. 2004. Predicting boron adsorption isotherms by Midwestern soils using the constant capacitance model. Soil Sci. Soc. Am. J. 68:795–801. doi:10.2136/sssaj2004.0795

Hayes, K.F., C. Papelis, and J.O. Leckie. 1988. Modeling ionic strength effects on anion adsorption at hydrous oxide/solution interfaces. J. Colloid Interface Sci. 125:717–726. doi:10.1016/0021-9797(88)90039-2

Hayes, K.F., A.L. Roe, G.E. Brown, K.O. Hodgson, J.O. Leckie, and G.A. Parks. 1987. In situ X-ray absorption study of surface complexes: Selenium oxyanions on α-FeOOH. Science (Washington, DC) 238:783–786. doi:10.1126/science.238.4828.783

Herbelin, A.L., and J.C. Westall. 1999. FITEQL: A computer program for determination of chemical equilibrium constants from experimental data. Rep. 99–01, Version 4.0. Dep. of Chemistry, Oregon State Univ., Corvallis.

Hiemstra, T., R.P.J.J. Rietra, and W.H. van Riemsdijk. 2007. Surface complexation of selenite on goethite: MO/DFT geometry and charge distribution. Croat. Chem. Acta 80:313–324.

Hiemstra, T., and W.H. van Riemsdijk. 1999. Surface structural ion adsorption modeling of competitive binding of oxyanions by metal (hydr)oxides. J. Colloid Interface Sci. 210:182–193. doi:10.1006/jcis.1998.5904

Jordan, N., C. Lomenech, N. Marmier, E. Giffaut, and J.-J. Ehrhardt. 2009a. Sorption of selenium(IV) onto magnetite in the presence of silicic acid. J. Colloid Interface Sci. 329:17–23. doi:10.1016/j.jcis.2008.09.052

Jordan, N., C. Lomenech, N. Marmier, E. Giffaut, and J.-J. Ehrhardt. 2009b. Competition between selenium(IV) and silicic acid on the hematite surface. Chemosphere 75:129–134. doi:10.1016/j.chemosphere.2008.11.018

Kim, S.S., J.H. Min, J.K. Lee, M.H. Baik, J.-W. Choi, and H.S. Shin. 2012. Effects of pH and anions on the sorption of selenium ions on the magnetite. J. Environ. Radioact. 104:1–6. doi:10.1016/j.jenvrad.2011.09.013

Lakin, H.W. 1961. Selenium content of soils. USDA-ARS Agric. Handb. 200. U.S. Gov. Print. Office, Washington, DC. p. 27–34.

Lee, S., J.J. Doolittle, and H.J. Woodard. 2011. Selenite adsorption and desorption in selected South Dakota soils as a function of pH and other oxyanion ions. Soil Sci. 176:73–79. doi:10.1097/SS.0b013e31820a0ff6

Lévesque, M. 1974. Selenium distribution in Canadian soil profiles. Can. J. Soil Sci. 54:63–68. doi:10.4141/cjss74-008

Manceau, A., and L. Charlet. 1994. The mechanism of selenate adsorption on goethite and hydrous ferric oxide. J. Colloid Interface Sci. 168:87–93. doi:10.1006/jcis.1994.1396

Martinez, M., J. Gimenez, J. de Pablo, M. Rovira, and L. Duro. 2006. Sorption of selenium(IV) and selenium(VI) onto magnetite. Appl. Surf. Sci. 252:3767–3773. doi:10.1016/j.apsusc.2005.05.067

Masscheleyn, P.H., R.D. Delaune, and W.H. Patrick. 1990. Transformations of selenium as affected by sediment oxidation-reduction potential and pH. Environ. Sci. Technol. 24:91–96. doi:10.1021/es00071a010

Missana, T., U. Alonso, and M. García-Gutiérrez. 2009. Experimental study and modelling of selenite sorption onto illite and smectite clays. J. Colloid Interface Sci. 334:132–138. doi:10.1016/j.jcis.2009.02.059

Neal, R.H., and G. Sposito. 1989. Selenate adsorption on alluvial soils. Soil Sci. Soc. Am. J. 53:70–74. doi:10.2136/sssaj1989.03615995005300010013x

Neal, R.H., G. Sposito, K.M. Holtzclaw, and S.J. Traina. 1987. Selenite adsorption on alluvial soils: I. Soil composition and pH effects. Soil Sci. Soc. Am. J. 51:1161–1165. doi:10.2136/sssaj1987.03615995005100050012x

Ohlendorf, H.M., D.J. Hoffman, M.K. Saiki, and T.W. Aldrich. 1986. Embryonic mortality and abnormalities of aquatic birds: Apparent impacts of selenium from irrigation drainwater. Sci. Total Environ. 52:49–63. doi:10.1016/0048-9697(86)90104-X

Papelis, C., G.E. Brown, G.A. Parks, and J.O. Leckie. 1995. X-ray absorption spectroscopic studies of cadmium and selenite adsorption on aluminum oxides. Langmuir 11:2041–2048. doi:10.1021/la00006a033

Parida, K.M., B. Gorai, N.N. Das, and S.B. Rao. 1997. Studies on ferric oxide hydroxides. III. Adsorption of selenite (SeO_3^{2-}) on different forms of iron oxyhydroxides. J. Colloid Interface Sci. 185:355–362. doi:10.1006/jcis.1996.4522

Peak, D. 2006. Adsorption mechanisms of selenium oxyanion ions at the aluminum oxide/water interface. J. Colloid Interface Sci. 303:337–345. doi:10.1016/j.jcis.2006.08.014

Peak, D., U.K. Saha, and P.M. Huang. 2006. Selenite adsorption mechanisms on pure and coated montmorillonite: An EXAFS and XANES study. Soil Sci. Soc. Am. J. 70:192–203. doi:10.2136/sssaj2005.0054

Rajan, S.S.S. 1979. Adsorption of selenite, phosphate and sulphate on hydrous alumina. J. Soil Sci. 30:709–718. doi:10.1111/j.1365-2389.1979.tb01020.x

Rovira, R., J. Giménez, M. Martínez-Lladó, J. de Pablo, V. Martí, and L. Duro. 2008. Sorption of selenium(IV) on the natural iron oxides: Goethite and hematite. J. Hazard. Mater. 150:279–284. doi:10.1016/j.jhazmat.2007.04.098

Sims, J.T., and F.T. Bingham. 1968. Retention of boron by layer silicates, sesquioxides, and soil materials: II. Sesquioxides. Soil Sci. Soc. Am. Proc. 32:364–369. doi:10.2136/sssaj1968.03615995003200030028x

Sposito, G. 1983. Foundations of surface complexation models of the oxide-aqueous solution interface. J. Colloid Interface Sci. 91:329–340. doi:10.1016/0021-9797(83)90345-4

Sposito, G., J.C.M. de Wit, and R.H. Neal. 1988. Selenite adsorption on alluvial soils: III. Chemical modeling. Soil Sci. Soc. Am. J. 52:947–950. doi:10.2136/sssaj1988.03615995005200040008x

Sprycha, R. 1989a. Electrical double layer at alumina/electrolyte interface. I. Surface charge and zeta potential. J. Colloid Interface Sci. 127:1–11. doi:10.1016/0021-9797(89)90002-7

Sprycha, R. 1989b. Electrical double layer at alumina/electrolyte interface. II. Adsorption of supporting electrolyte ions. J. Colloid Interface Sci. 127:12–25. doi:10.1016/0021-9797(89)90003-9

Su, C., and D.L. Suarez. 2000. Selenate and selenite sorption on iron oxides: An infrared and electrophoretic study. Soil Sci. Soc. Am. J. 64:101–111. doi:10.2136/sssaj2000.641101x

Wijnja, H., and C.P. Schulthess. 2000. Vibrational spectroscopy study of selenate and sulfate adsorption mechanisms on Fe and Al (hydr)oxide surfaces. J. Colloid Interface Sci. 229:286–297. doi:10.1006/jcis.2000.6960

Zhang, P., and D.L. Sparks. 1990. Kinetics of selenate and selenite adsorption/desorption at the goethite/water interface. Environ. Sci. Technol. 24:1848–1856. doi:10.1021/es00082a010